This document is confidential and is proprietary to the American Chemical Society and its authors. Do not copy or disclose without written permission. If you have received this item in error, notify the sender and delete all copies.

Extreme molecular complexity resulting in a continuum of carbonaceous species in biomass burning tar balls from wildfire smoke

Journal:	ACS Earth and Space Chemistry
Manuscript ID	sp-2021-00141y.R1
Manuscript Type:	Article
Date Submitted by the Author:	27-Aug-2021
Complete List of Authors:	Brege, Matthew; Michigan Technological University, Chemistry China, Swarup; Pacific Northwest National Laboratory, EMSL Schum, Simeon; Michigan Technological University, Chemistry Zelenyuk, Alla; Pacific Northwest National Laboratory, Chemical Physics & Analysis Mazzoleni, Lynn; Michigan Technological University, Department of Chemistry

SCHOLARONE™ Manuscripts Extreme molecular complexity resulting in a continuum of carbonaceous species in biomass burning tar balls from wildfire smoke

Matthew A. Brege*1, Swarup China2, Simeon Schum1, Alla Zelenyuk2, Lynn R. Mazzoleni1

¹Department of Chemistry, Michigan Technological University, Houghton, MI 49931 USA

²Pacific Northwest National Laboratory, Richland, WA 99354 USA

KEYWORDS: aerosol, biomass burning, tar balls, ultrahigh resolution mass spectrometry, molecular characterization.

ABSTRACT: Biomass burning emits a wide range of carbonaceous particles into the atmosphere and has negative impacts on human health and the Earth's radiative balance. Nonvolatile spherical organic aerosol particles, commonly known as tar balls, represent one of the most abundant particles in aged biomass burning smoke. However, the detailed molecular-level composition of ambient tar balls is largely unknown but critical to access their environmental impacts. Ambient aerosol samples collected during a wildfire event, which were ~90% tar balls by number fraction, were analyzed using ultrahigh resolution Orbitrap Elite mass spectrometry with four complementary ionization modes. Our results show the molecular composition of tar balls to be complex, composed of over 10,000 molecular formulas. Model estimated saturation mass

concentrations and relative humidity dependent glass transition temperatures were consistent with low volatility and solid morphology as expected for tar balls. Room-temperature evaporation kinetics showed that these particles retained ~90% of their volume after 24 h of evaporation. The molecular complexity detected here signifies a continuum of carbonaceous species, ranging from C₃ to C₄₅ with continuous ranges of oxygenation and hydrogen saturation for each C_n. Approximately 24% of molecular formulas were estimated to be highly aromatic, which could indicate chemical compounds with negative health effects, and which may contribute to visible light absorption. The carbon continuum observed here has significant implications for the molecular characterization of atmospheric organic matter. The level of complexity detected here should not be ignored in future studies and we demonstrate that multiple analytical methods may be required to suitably interpret this complexity on a molecular level.

1. INTRODUCTION

Wildfires in North America have steadily increased in frequency and duration and are attributed to drier conditions brought on by increasing global temperatures.^{1, 2, 3} The extreme temperatures of wildfires can create convective forces capable of elevating some of the emissions into the free troposphere and the stratosphere, facilitating long range transport.^{4, 5, 6} In addition to wildfires, residential biomass burning for heating and cooking are significant source of carbon compounds to the atmosphere^{7, 8, 9} because an estimated 75% of the world's population uses wood as a fuel source.⁵ Primary organic aerosol emissions are introduced directly to the atmosphere in the particle phaser, while gas phase emissions can be transformed by atmospheric oxidants into lower volatility species, which can undergo gas-to-particle phase conversion. These processes can lead to the formation of new particles or condensation on pre-existing particles, collectively referred to as

secondary organic aerosol. 10, 11 Both primary and secondary organic aerosol particles impose significant risks to human health and global climate.^{5, 12, 13} Biomass burning emissions include mutagenic nitro-phenols¹⁴ and carcinogenic polycyclic aromatic hydrocarbons (PAHs), ^{15, 16} additionally the catalytic generation of reactive oxygen species has been associated in particular with biomass burning aerosol and humic-like substances. 17, 18 Prolonged exposure to fine particulate matter is associated with cardiovascular and pulmonary diseases. 12 Light absorbing "black carbon" and "brown carbon" contribute to atmospheric warming and are associated with biomass burning emissions. ^{19, 20, 21} The total absorption of biomass burning aerosol is a product of the mixture of chemical components, 21, 22, 23, 20 with a wide range of wavelength dependencies observed. 21, 24, 25 Black and brown carbon present in different fractions of total aerosol mass both contribute to the total absorption observed for biomass burning aerosol.^{21, 20} Black carbon has a larger absorption potential but is present in smaller mass fractions, while brown carbon is present in larger mass fractions but has less absorptive potential. 19, 26, 21 Reduction strategies which focus on absorbing aerosol may help to mitigate the effects of climate change in as little as 5 years.²⁷ This is largely because the energy absorption potential for black and brown carbon aerosol is much greater than an equivalent mass of atmospheric CO₂, while also having much shorter projected atmospheric lifetimes. 13, 28

Organic spherical particles commonly known as "tar balls", are a morphologically defined subset of atmospheric aerosol primarily produced in the smoldering phase of biomass burning.²⁹ Tar balls are highly viscous low-volatility glass-like particles approximately 100 to 300 nm in size, with no observable condensation nuclei or concentric layers.^{29, 30, 31} Tar balls can resist the high-powered electron beam of microscopy techniques while other organic particles are partially or fully vaporized.³² In wildfires, tar balls have been observed in much greater numbers relative to soot

particles, at an abundance of approximately 10:1.^{33, 34, 31} Tar balls are not directly emitted, but increase in occurrence downwind of biomass burning plumes, which indicates they are formed over a matter of hours as the plume ages.^{31, 35} The detailed molecular level mechanisms for the formation of tar balls is still unknown, where the relative contributions of gas-to-particle-phase reactions and particle phase oligomerization reactions to their formation is unclear. Tar balls contain light absorbing brown carbon³³ and optically "dark" and "light" tar balls have been observed.³⁴ A wide range of wavelength dependent light absorption has been described in the literature^{36, 33, 37} implying that the molecular makeup of tar balls from different sources may vary.

The chemical characterization of tar balls is an active area of research given their high abundance in biomass burning smoke and light absorption properties. Compared to liquid and gas phase fuels, the combustion of solid fuels, such as wood in biomass burning, leads to an enhanced degree of complexity in the resulting molecular byproducts.³⁸ Lignin, a biopolymer, constitutes approximately 30% of wood tissue and many wood burning products have chemical structures related to the phenolic monomers which make up lignin.^{7,29} The diversity of chemical products is highly dependent on the combustion conditions of the fire, including fuel type, moisture content, fire size, oxygen availability and the progression of flaming versus smoldering phases.^{5,29,38} Broad classifications of chemical species are associated with biomass burning emissions, including alcohols, aldehydes, ketones, carboxylic acids, esters, ethers, furans, sugars and anhydro-sugars, lignans, quinones, nitro-aromatics and PAHs.^{5,7,24,39,40,41} Particularly for tar balls, methoxy, ketone and carboxylic acid functional groups are expected with influence from aromatic and phenolic structures.^{35,42} Transmission electron microscopy and energy-dispersive X-ray spectroscopy analyses describe elemental compositions of primarily carbon and oxygen.^{33,34} A

recent study by Adachi et al.³⁵ describes the importance of organic nitrogen compounds in the formation of tar balls, expected to be in the form of organic nitrate and nitro-aromatic species.

The molecular level characterization of tar balls has the same analytical challenges as any other complex mixture of organics. In recent years analytical approaches using ultrahigh-resolution mass spectrometry have become highly valuable in analyzing these types of mixtures, because of their ability to efficiently resolve the isobaric ions of chemical species with the same nominal mass. 43, ⁴⁴ These "bottom-up" style analyses for complex mixtures are often implemented because analytical standards for comparison are nonexistent. "Soft-ionization" techniques like electrospray ionization (ESI) produce charged analytes with little to no fragmentation. 45 When combined with ultra-high resolution techniques ESI has been used successfully to reveal the molecular complexity of ambient organic aerosol. 46, 47, 48, 49, 50, 51, 52, 53 ESI is selective to molecules with polar functional groups capable of easily accepting or removing a hydrogen ion. 45 Molecules without these polar groups can have suppressed ionization due to the competitive nature of ionization. Atmospheric pressure photoionization (APPI) is an alternate soft ionization method with increased sensitivity to low polarity and aromatic molecules with respect to ESI.⁵⁴ In this study, the acetonitrile-soluble extracts of two biomass burning samples heavily influenced by tar ball morphology were analyzed using ultrahigh-resolution Orbitrap Elite mass spectrometry (OTE-MS). We have applied an extensive molecular level analysis using the negative and positive polarities of ESI and APPI, hereafter abbreviated as -APPI, +APPI, -ESI, and +ESI. The observed result is an unprecedented degree of molecular complexity. We will show how this combination of ionization techniques provides a more comprehensive view of the complex mixture of organic matter in atmospheric aerosol and demonstrates a continuum of carbonaceous chemical species in organic aerosol.

2. METHODS

2.1 MASS SPECTROMETRY ANALYSIS

In 2017 several wildfires burned in the Pacific Northwest near central Washington.⁵⁵ Two aerosol filter samples were collected at the Pacific Northwest National Lab (Richland, WA) on 5-Sep 2017 and 6-Sep 2017 and will be referred to here as BB05 and BB06, respectively. HYSPLIT back trajectories show a major influence from northern Washington for the preceding 48 hours before sample collection (Fig. S1). The samples were collected on 90 mm PTFE filters by drawing air at 80 L min⁻¹ for 6 hours (a sample blank was also prepared).

High purity analytical grade solvents were used in every step of sample preparation. A portion of the aerosol filter was extracted in acetonitrile (ACN), a polar organic aprotic solvent, using a low-speed orbital shake table for 90 minutes at 60 RPM. The extract was filtered using a preconditioned 0.2 um PTFE membrane syringe filter to remove insoluble matter. ACN was used in an effort to extract the low-polarity organics which are not water-soluble and are expected to be present in tar balls.⁵⁶ The results described here are thus limited to those chemical species which are extracted by ACN.

The samples were analyzed using OTE-MS in the Chemical Advanced Resolution Methods (ChARM) Laboratory at Michigan Technological University (Houghton, Michigan, USA). Samples were directly infused into the instrument using a 250 µL syringe pump at 5 to 30 µL min⁻¹. The analyses used APPI and ESI in both the positive and negative polarities. Briefly, APPI uses photolytic ionization via a krypton UV lamp, and is expected to ionize molecules with lower polarity and increased aromatic character. ESI uses a charged capillary to create a fine spray of evaporating solvent, while also applying a charge, and is expected to ionize acidic and basic polar organics. For the +APPI and -APPI analysis a vaporizer temperature of 450 °C was used, and the

samples were diluted by a factor of 2 with 1% toluene added as a dopant for the UV lamp.⁵⁴ The samples were diluted by a factor of 4 for -ESI and by a factor of 8 for +ESI to optimize the ion signal. Data was collected for 200 scans over the range of m/z 100 to 800 and at a resolution of 240,000 (defined at m/z 400) with spectrum averaging.

Mass lists were generated from an average of the 200 scans using Xcalibur software (Thermo Scientific v. 3.0). The newly developed MFAssignR⁵⁷ was used to estimate the noise threshold, recalibrate the spectra and assign molecular formulas to the measured masses. A series of custom R scripts (R v. 3.5.1 and RStudio v. 1.1.463) were used to perform blank subtraction and ensure data quality. The process for molecular formula assignment using MFAssignR is beyond the scope of this paper and described elsewhere⁵⁷. A detailed synopsis of formula assignment using MFAssignR for this data set is provided in section S1 of the supplemental text. Briefly, molecular formulas were assigned allowing for carbon, hydrogen, oxygen, nitrogen and sulfur elements with limits placed on oxygen (0 to 30), nitrogen (0 to 3) and sulfur (0 to 1). Up to one sodium ion was allowed for data collected in +ESI to allow for positively charged sodium adducts in addition to hydrogen adducts. Formulas were further validated by a series of rigorous quality assurance steps as in our previous work^{58, 59} (see section S1.4 of the supplemental text). The reconstructed mass spectra of BB05 using our comprehensive multi-ionization OTE-MS analysis are shown in Fig. S3. In each ionization mode we observed ~4000 to 7000 formulas and a total of ~10,000 formulas in each sample after accounting for formulas which were detected in multiple ionization modes. Section S3 of the supplemental text defines 15 orthogonal fractions to describe the different overlapping ionization methods which molecular formulas may have in common. These fractions are displayed graphically in Figs. S16 and S17, where it can be seen there were a significant number of formulas observed in each fraction. Overall, there was good agreement between the two

samples with respect to the number of molecular formulas detected with each ionization method (Figs. 1 and S4). The combined analysis identified ~12,000 total molecular formulas for biomass combustion tar balls accounting for formulas observed in both samples. ESI and APPI are non-quantitative techniques which are selective for different chemical species. Thus, to avoid misrepresenting high ionization efficiency for high abundance in the samples, our discussion involves the observed numbers of molecular formulas without accounting for abundance in the mass spectra.

2.2 MOLECULAR FORMULA CLASSIFICATION

The accepted molecular formulas were classified into five elemental groups: "CH", "CHO", "CHN", "CHNO" and "CHOS", based on the respective inclusion of carbon, hydrogen, oxygen, nitrogen and sulfur elements in the formula. We note that each identified molecular formula likely represents multiple different structural isomers at extremely small concentrations^{60, 61} and that complete chemical structural elucidation is impossible without chromatographic separation and additional tandem mass spectrometry (MSⁿ) analysis. The elemental composition of the molecular formulas can be used to estimate chemical properties through calculations, such as the double bond equivalents (DBE), which represent the level of "unsaturation", i.e., the number of double bonds + ring moieties present. The modified aromaticity index (AI_{mod})^{62, 63} was used to estimate the number of carbon-carbon unsaturated bonds (aromatic character). Molecular formulas were separated into four groups based on their calculated AI_{mod} value: 1) aliphatic: $AI_{mod} = 0$; 2) olefinic: $0 < AI_{mod} \le 0.5$; 3) aromatic: $0.5 < AI_{mod} \le 0.67$; 4) condensed aromatic: $AI_{mod} > 0.67$. For condensed aromatics, we also required formulas to have 8 or more carbon atoms $(C_n \ge C_8)$ to avoid the misclassification of formulas which do not have a reasonable number of carbon atoms to form multiple ring structures. The average oxidation state of carbon (OS_C) was estimated as described

by Kroll et al.⁶⁴ The calculations for DBE, AI_{mod} and OS_C are described in detail in the supplemental text with equations (S3) to (S8).

The volatility of the molecular formulas, specifically the saturation mass concentration (C_0 in units of ug m⁻³) was estimated using a model developed by Li et al. ⁶⁵ Molecular formulas were separated into five groups based on their calculated C_0 values: 1) volatile organic compounds (VOC): $C_0 >$ $3x10^6$; 2) intermediate volatility organic compounds (IVOC): $300 < C_0 \le 3x10^6$; 3) semi-volatile organic compounds (SVOC): $0.3 < C_0 \le 300$; 4) low-volatility organic compounds (LVOC): $3x10^ ^4 < C_0 \le 0.3$; 5) extremely low-volatility organic compounds (ELVOC): $C_0 \le 3x10^{-4}$. In addition to the calculated volatility of the molecular formulas, the volatility of overall particles was determined using measurements of room-temperature evaporation kinetics of size-selected particles, described in detail elsewhere. 66 The relative humidity dependent glass transition temperature (T_{g,RH}) was estimated for CHO formulas based on the work of DeRieux et al.⁶⁷ The ratio of T_{g,RH} to the average ambient temperature (T_{amb}) during sample collection (Table S1) can be used to estimate the phase state ratio (PSR) of the molecular formulas as defined in DeRieux et al.⁶⁷ The molecular formulas were separated into three groups based on the calculated PSR: 1) solid: $PSR \ge 1$; 2) semi-solid: $0.8 \le PSR < 1$; 3) liquid: PSR < 0.8. The equations and parameters used to calculate C₀ and T_{g,RH} are described in detail in the supplemental text with equations (S9) to (S13).

3. RESULTS AND DISCUSSION

3.1 SINGLE PARTICLE ANALYSIS OF TAR BALLS

Single particle analysis using scanning electron microscopy (SEM) and energy dispersive X-ray spectroscopy of the filter samples suggest that tar balls were the most abundant particle type

collected on the sample filters (~90% number fraction). Tilted view images of particles show spherical morphology, suggesting the solid state of these particles (Fig. 2A). Similarly, real-time characterization of individual aerosol particles using a single particle mass spectrometer (miniSPLAT⁶⁸) indicated that the vast majority (>95%) of sampled aerosol particles were spherical biomass burning particles, i.e., tar balls. Scanning transmission X-ray microscopy (STXM) and near-edge X-ray absorption fine structure (NEXAFS) spectra of the particles (Fig. 2B) agree with previous results described for tar balls; absorption peaks observed at 285.1, 286.7 and 288.5 correspond to aromatic/phenolic, ketone/carbonyl and carboxylic acid functionalities. ⁶⁹ In addition to filter sampling for offline analysis, online particle characterization was conducted using a scanning mobility particle sizer (SMPS) and miniSPLAT. Real time measurements of particle size distributions, density, shape, mass loadings, single particle mass spectra, and volatility were obtained.⁶⁶ The average size distributions of BB05 and BB06 are shown in Fig. S2 and using the measured density of 1.4 g cm⁻³ yields an average aerosol mass loading of $170 \pm 30 \,\mu g \, m^{-3}$. The room-temperature evaporation kinetics of size-selected aerosol particles (150 nm, 234 nm and 311 nm) were measured for BB05 (Fig. 2C). Overall, the particles lost only ~10% of their volume after 24 h of evaporation in an organic-free environment, implying that the particle composition is dominated by nearly non-volatile organic compounds ($C_0 \le 10^{-4} \, \mu g \, m^{-3}$).

3.2. MOLECULAR COMPOSITION OF TAR BALLS

Comprehensive OTE-MS exact mass measurements were performed on the ACN-soluble fraction of ambient aerosol heavily influenced by tar ball morphology, as defined by SEM and miniSPLAT analyses. OTE-MS analysis identified a predominance of CHO and CHNO molecular formulas with minor contributions from the CH, CHN and CHOS groups (Fig. S5). The large number of CHNO species observed here (~50% of formulas per sample) is consistent with a recent chemical

characterization of tar balls which suggest the presence of organonitrates.³⁵ A summary of BB05 and BB06 molecular formulas by elemental group is provided in Tables 1 and 2 respectively. An overall continuum of carbonaceous chemical species was observed from the vast number of molecular formulas detected. The molecular formulas are continuous from C₃ to C₄₅ with continuous ranges of oxygenation and hydrogen saturation (represented by DBE values) for each C_n. These trends can be observed in the DBE *vs.* carbon number space (Figs. 3 and S6) accompanied by distribution histograms of DBE and carbon number on the respective axes.

The calculated AI_{mod} values for the molecular formulas coincide well with the observed DBE and carbon number trends in this space. Formulas with low carbon numbers (~C₃ to C₁₀) and low DBE (~0 to 5) are predicted to be mostly aliphatic and olefinic species, while formulas with high DBE (~15 to 20) and moderate carbon numbers (~C₂₅ to C₃₅) are predicted to be mostly aromatic and condensed aromatic species. Oxygenation was the most intense for formulas between $\sim C_{20}$ to C_{30} , while overall the upper limit in oxygenation increased with carbon number. Formulas with C₃₀ to C₄₅ had consistently higher oxygen number distributions compared to formulas with C₃ to C₁₀. This enhanced oxygenation should be expected for larger molecules as there are more opportunities for the addition of reactive species, especially considering we see more carboncarbon bond saturation (represented by AI_{mod}) in formulas with higher carbon numbers. Given the overall low level of observed oxidation in these molecular formulas (average O/C of ~0.36) the presence of higher molecular weight oxygenated species is a point of interest. The area of highest molecular formula density in this space is located from approximately C_{14} to C_{26} and DBE 8 to 14. These molecular formulas trend well with the overall observed characterization for the samples; the formulas are predominantly CHNO followed closely by CHO species, with AI_{mod} values that predict mostly olefinic and some of aromatic species. We observe low numbers of formulas at extremely low DBE (0 to 3) especially for carbon numbers above C_{10} . As these species would be expected to be extremely aliphatic and low polarity, we would not expect them to be extracted by ACN. At higher carbon numbers (C_{35} to C_{45}) and higher DBE values (15 to 20) we also observe few molecular formulas, which we expect would be condensed aromatic species and similarly insoluble in ACN.

Our results show a strong overlap in the chemical characteristics of molecular formulas across multiple ionization modes. These results differ from previously published work analyzing atmospheric aerosol samples via multiple ionization methods⁷⁰ and the disparity may be attributed to the differences in sample extraction solvent or possibly the chemical nature of the different samples between the two studies. Nevertheless, approximately 16% of formulas were detected in all four ionization modes, with approximately 24%, 15%, 6% and 2% being observed exclusively in +ESI, -ESI, +APPI and -APPI, respectively. The majority of molecular formulas in this study were detected in 2 or 3 of the used ionization modes. The distribution of molecular formulas observed exclusively in one ionization mode are consistent with the expectations for these methods (Figs. 1 and S4)^{71, 54, 56}. Formulas exclusive to -ESI were shifted to higher O/C (more oxidized), while those exclusive to +ESI were shifted to lower O/C (less oxidized). Formulas exclusive to -APPI had moderate O/C and were shifted to lower H/C (more unsaturated) and those exclusive to +APPI were shifted to lower O/C and lower H/C (less oxidized and more unsaturated). Compared to previous studies of aerosol using only negative mode ESI, 58, 59 the combination of these four ionization methods identifies 3 to 5 times the numbers of molecular formulas. This enhanced examination allows for the observation of a continuum of carbonaceous species in the complex mixture of organic aerosol.

The carbon continuum extends from aliphatic into the aromatic and condensed aromatic chemical space with proportionately high DBE values over the entirety of the observed carbon numbers. Many of the molecular formulas have AI_{mod} values defined for olefinic species while a notable number had AI_{mod} values suggesting an aromatic or condensed aromatic structure (Fig. S7). The average O/C ratio for the molecular formulas of BB05 was 0.36 ± 0.23 and slightly higher in BB06 with 0.37 ± 0.23 . Based on the limits described in Tu el al. ⁷² an overwhelming majority of the molecular formulas have low to moderate oxygenation and oxidation, as shown by the distributions of formulas in Figs. 1 and S4, both to the left of the vertical O/C = 0.6 line and above the diagonal OS_C = 0 line. Although many of the molecular formulas were common to both samples, those formulas exclusively observed in BB06 compared to those exclusively observed in BB05 had slightly higher H/C (1.42 \pm 0.41 vs. 1.22 \pm 0.35) and O/C (0.35 \pm 0.23 vs. 0.32 \pm 0.26), indicating a slight enhancement in the atmospheric aging of BB06 Fig. S8). These differences in oxidation are consistent with the shift towards larger particle sizes in BB06 (Fig. S2). The low oxygenation and high aromatic character observed here suggest the samples had an overall minimal influence of atmospheric aging, possibly explained by the high viscosity expected for tar balls and thus slow diffusion of atmospheric oxidants into the particles. 73, 30, 59

3.3. VOLATILITY OF TAR BALL MOLECULAR SPECIES

A majority of molecular formulas had estimated saturation mass concentrations (C_0) using the Li et al.⁶⁵ model classified as either LVOC or ELVOC (Fig. S9). The values for estimated C_0 ranged from approximately 7.0×10^{-18} to 2.6×10^7 µg m⁻³ and the distribution of molecular formulas towards lower C_0 (Figs. 4 and S10) was in good agreement with the measured room-temperature evaporation kinetics for BB05. The calculated $T_{g,RH}$ values ranged from 152.6 to 378.5 K with the majority of CHO formulas in both samples being distributed towards higher $T_{g,RH}$ (Figs. 4 and

S10). There were noticeable differences in the calculated $T_{g,RH}$ values for CHO molecular formulas observed in APPI compared to ESI, where the APPI formulas were shifted towards lower $T_{g,RH}$. This is especially noticeable in the formulas exclusive to an ionization method (upper panel of Figs 4 and S10) particularly for +APPI exclusive formulas. Molecular species expected to be more liquid-like (PSR < 0.8) would also be expected to have higher vapor pressure than solid species, which could lead to enhanced vaporization and detection via the APPI methods.

Based on the calculated ratios of $T_{g,RH}$ to T_{amb} , a majority of CHO formulas observed in both BB05 and BB06 are anticipated to be highly viscous (Fig. S11). These results suggest that the tar balls collected in these two samples were solid spheres, however we note the limits of the model used to calculate $T_{g,RH}$, which currently does not account for the significant influence CHNO species observed in these samples. The relationships between the estimated volatility, calculated $T_{g,RH}$ and molecular weight for BB05 and BB06 are shown in Figs 4 and S10 respectively. The carbon continuum appears to follow the expected trend of decreasing volatility with increasing $T_{g,RH}$ for increasing molecular weight. Formulas with higher $T_{g,RH}$ are anticipated to be in a semi-solid or solid state, as their $T_{g,RH}$ approach and exceed T_{amb} . Approximately 80% of the observed CHO molecular formulas in both BB05 and BB06 were classified as LVOC or ELCOV (estimated $C_0 < 0.3$) and expected to be semi-solid or solid ($T_{g,RH} > 250$ K with $T_{amb} \approx 300$ K), which is consistent with the expectation of low volatility and glassy-like phase states for tar balls.

4. IMPLICATIONS OF MOLECULAR COMPLEXITY

4.1 HEALTH IMPLICATIONS

The catalytic generation of reactive oxygen species such as peroxides, superoxide anion and hydroxyl radical, have been associated with biomass burning aerosol and humic-like substances¹⁸

and aromatic quinones and quinone-like species. ¹⁷ Reactive oxygen species can cause oxidative stress in living organisms, making them, and by association biomass burning emissions, a serious health hazard. We observe a significant number of aromatic and condensed aromatic species with low to moderate oxidation (O/C < 0.6) in our samples (Figs. 1, S4 and S12) where quinones and quinone-like species are possible.

Metabolic processing and oxidation of biomass burning emissions, such as PAH species, could catalyze the production of reactive oxygen species 16 and we expect many of the condensed aromatic species observed here could be related to PAHs. Lin et al. 70 report the observation of molecular formulas in biomass burning samples which are likely to be PAHs, using a mix of extremely low-polarity extraction solvents. We do not observe any CH group molecular formulas with high enough AI_{mod} to indicate hydrocarbon PAHs. However, we do observe many CHO, CHN and CHNO species which are possibly functionalized oxo-PAHs and nitro-PAHs, with ring embedded heteroatoms also being possible. Functionalized PAH derivatives have been previously observed in aerosol, attributed to biomass burning sources. 41, 74, 70 While the specific carcinogenic effects of oxygen and nitrogen functionalized PAHs are still somewhat uncertain, in general terms, the negative health effects of PAHs occur once they have been oxidized within the biological system, allowing for polar interactions with cellular macromolecular structures like DNA and proteins. 16 Functionalized PAHs would have increased polar character and water solubility, and thus the potential to be more biologically available for hazardous interactions than their hydrocarbon PAH counterparts.

A noticeable number of CHNO aromatic species observed here had high O/N ratios, making nitrophenols and lignan-like oligomers possible. Many functionalized nitro-benzene compounds have known mutagenic effects⁷⁵ and it is possible that exposure to biomass burning emissions like tar

balls include these compounds. Considering the observed carbon continuum of these samples, it is likely that exposure to the aromatic and condensed aromatic species described here for tar balls poses a significant health risk. 17, 18, 74

4.2 ATMOSPHERIC IMPLICATIONS

A significant fraction of molecular formulas had calculated AI_{mod} values which describe aromatic or condensed aromatic character. Overall O/C ratios were low in conjunction with this high estimated aromatic character, making the potential for conjugated carbon-carbon bond structures which lead to light absorption possible. The previously described oxo-PAHs, nitro-PAHs, nitro-phenols and lignan-like oligomers with deleterious health effects would also be expected to be light absorbing. These types of aromatic and nitro-aromatic formulas are consistent with what would be expected of light absorbing species which contribute to atmospheric brown carbon. ^{76, 77, 78, 42} The slow evaporation kinetics for the collected aerosol particles (Fig. 1C), the low calculated viscosity and volatility of the molecular formulas (Fig. 4), and the observed low O/C ratio for molecular formulas, suggest that tar balls may be resistant to oxidative degradation and may persist in the atmosphere for some time. As wildfires are expected to increase in severity in North America with rising global temperatures^{1, 2, 3} the elevated emissions of tar balls may contribute to further atmospheric warming in a positive feedback loop from the production of absorbing aerosol.

4.3 FURTHER COMPLEXITY

The observed carbon continuum is consistent with the wide range of molecular formula compositions in several other atmospheric aerosol studies.^{47, 79, 49, 80, 51, 52, 81, 58, 59} It is likely that the observed carbon continuum is still incomplete and that the organic fraction of atmospheric aerosol is even more complex than described here. These results are influenced by both the ACN extraction

technique for the aerosol filters, as well as the ionization methods used for analysis. Additional extraction methods using a polar solvent like water or a low polarity solvent like hexane could be performed to isolate different chemical species which were not extracted here by ACN. Compared to our previous ^{51, 58, 59}, the inclusion of additional ionization modes resulted in an increase of 3-5 times the number of observed molecular formulas for ambient atmospheric aerosol samples. Additional ionization methods (such as atmospheric pressure chemical ionization) or the preseparation of samples before analysis by liquid chromatography may also reveal additional layers of complexity to this carbon continuum. In particular, positive and negative ionization modes should both be considered in future studies of similar ambient samples, as it is a straightforward process to change the polarity of a mass spectrometer without further modification of a given instrument. Considering that each molecular formula observed is likely composed of several different isomeric species^{61, 60} it is likely that the organic fraction of atmospheric aerosol is far more complex than any one analytical technique can reveal.

Table 1. BB05 molecular formula assignment summary.

	Table 1. BB03 molecular formula assignment summary.								
	Source	APPI				ESI			
Negative mode	Group	All	CHO	O (CHNO	All	СНО	CHNO	CHOS
	DBEa	10.28	10.3	31	10.23	9.19	9.53	9.35	2.29
	O/Ca	0.38	0.36	5 ().40	0.51	0.46	0.54	0.85
	H/C ^a	1.07	1.12	2 1	1.02	1.18	1.18	1.13	1.71
	Cna	19.42	20.9	93]	17.46	19.41	20.91	18.18	8.66
	Ona	6.78	6.98	3 (5.52	9.27	9.31	9.46	6.53
	N^b	4222	238	7 1	1835	5453	3146	2107	200
	Common	A DDI							
	Source	APPI				ESI			
e	Group	APPI	СНО	CHNO	СН	ESI All	СНО	CHNO	CHN
ode			CHO 10.28	CHNO 9.99	CH 4.64		CHO 9.04	CHNO 8.73	CHN 5.97
e mode	Group	All				All			
tive mode	Group DBE ^a	All 10.13	10.28	9.99	4.64	All 8.85	9.04	8.73	5.97
ositive mode	Group DBE ^a O/C ^a	All 10.13 0.29	10.28 0.27	9.99 0.32	4.64 0.00	All 8.85 0.29	9.04 0.34	8.73 0.25	5.97 0.00
Positive mode	Group DBE ^a O/C ^a H/C ^a	All 10.13 0.29 1.11	10.28 0.27 1.14	9.99 0.32 1.07	4.64 0.00 1.31	All 8.85 0.29 1.31	9.04 0.34 1.30	8.73 0.25 1.32	5.97 0.00 1.25

^aValues represent mathematical averages based on formula assignment. ^bValues represent the respective number of molecular formulas.

Table 2. BB06 molecular formula assignment summary.

	Source	APPI			ESI			
Negative mode	Group	All	СНО	CHNO	All	СНО	CHNO	CHOS
	DBE ^a	9.58	9.02	10.24	9.11	9.39	9.29	2.31
	O/Ca	0.38	0.37	0.38	0.50	0.46	0.54	0.90
	H/C ^a	1.13	1.21	1.04	1.19	1.19	1.14	1.69
	Cna	19.17	20.16	18.01	19.31	20.82	18.16	8.14
	Ona	6.70	6.93	6.44	9.19	9.20	9.38	6.59
	N ^b	4135	2222	1913	5415	3033	2201	181
	Source	APPI			ESI			
Positive mode	Group	All	СНО	CHNO	All	СНО	CHNO	CHN
	DBEa	9.44	9.51	9.35	8.42	8.69	8.20	5.72
	O/Ca	0.30	0.28	0.33	0.31	0.34	0.27	0.00
	H/Ca	1.15	1.18	1.11	1.34	1.34	1.34	1.28
	Cna	19.21	21.14	17.03	22.05	24.32	20.01	9.78
	Ona	5.37	5.41	5.32	6.49	7.81	5.30	0.00
	N^b	4730	2514	2216	7213	3564	3584	65

^aValues represent mathematical averages based on formula assignment. ^bValues represent the respective number of molecular formulas.

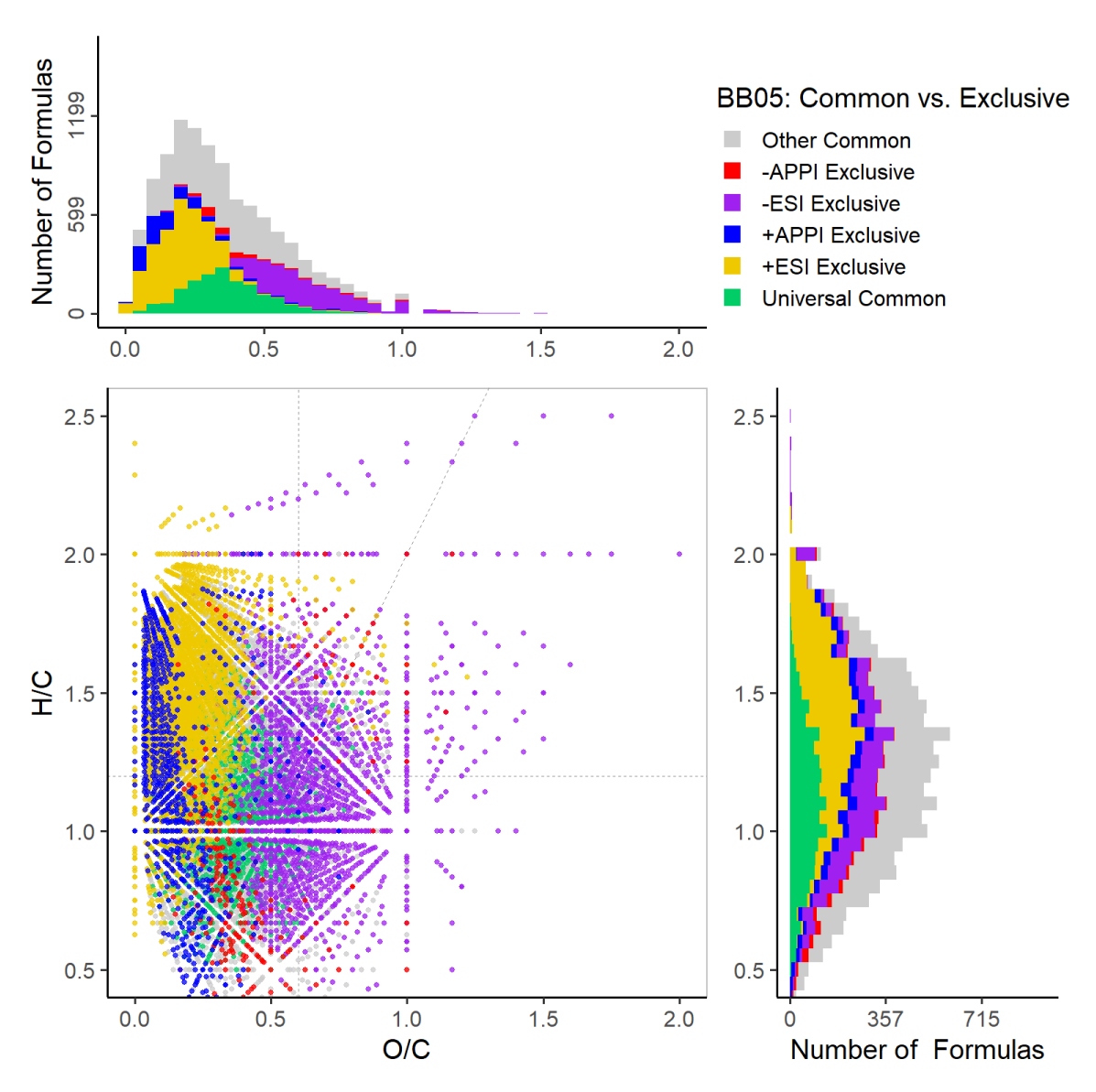
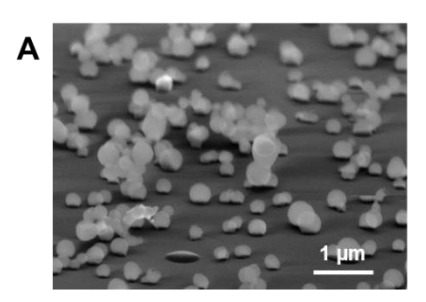
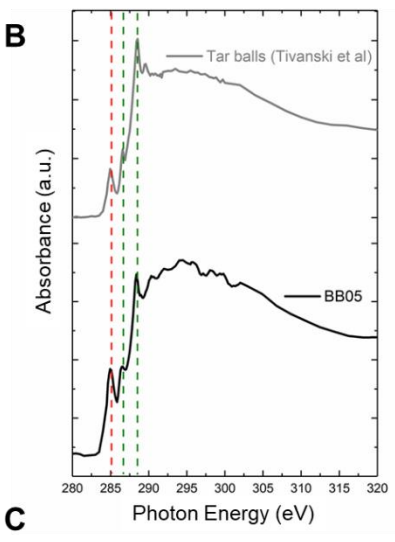


Figure 1. The distribution of all 10,887 molecular formulas of BB05 in van Krevelen space (center) with the density distribution of the formulas by O/C and H/C (top and right respectively) in order to visualize the magnitude of overlapping points in the center panel. Points (and bars) are colored by the method of detection, whether a formula was exclusive to one of the four ionization modes (red, purple, blue, gold) detected in all four modes (green) or some other combination of multiple ionization modes (gray). The total number of formulas are stacked in the density distribution plots. Dashed lines represent H/C = 1.2 (vertical), O/C = 0.6 (horizontal) and $OS_C = 0$ (diagonal).





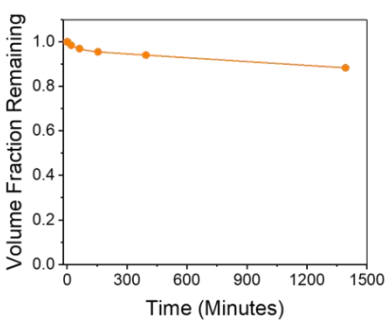


Figure 2. A) Scanning electron microscopy image of the aerosol filter sample collected 5-Sep 2017 (BB05). Tar balls were the most abundant particle type collected on the filter sample (~85-95% number fraction). B) Near-edge X-ray absorption fine structure (NEXAFS) spectra of BB05 filter collected particles. The absorption peaks observed at 285.1, 286.7 and 288.5 (dashed lines) agree with previous results described for tar balls (See section 3.1). C) The measured room-temperature evaporation kinetics of sizeselected aerosol particles (150, 234 and 311 nm) for BB05. The particles lost ~10% of their volume after 24 h (1,440 min) of evaporation in an organic-free environment.

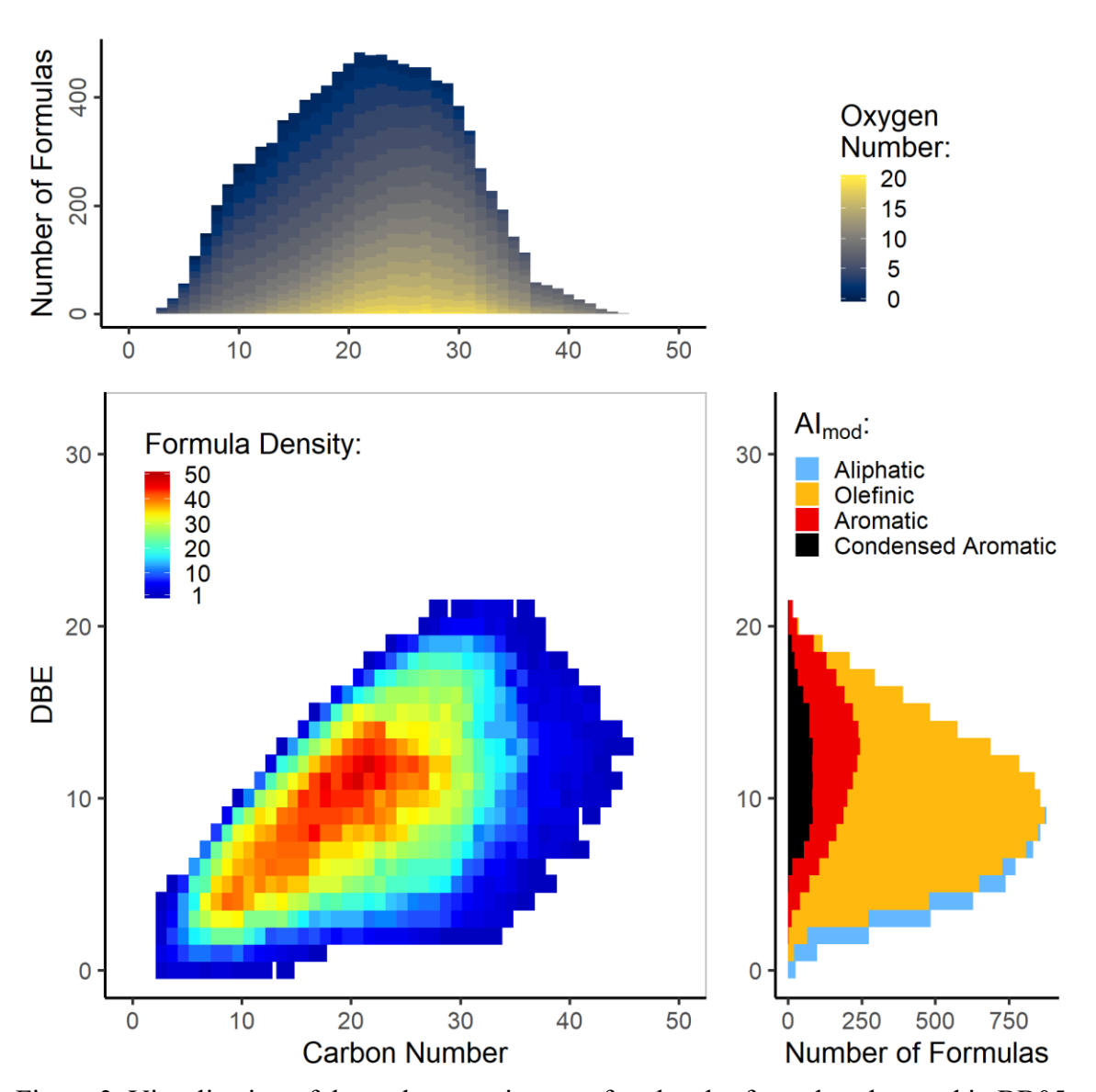


Figure 3. Visualization of the carbon continuum of molecular formulas observed in BB05. The distribution of molecular formulas is shown in the double bond equivalents (DBE) vs. carbon number space (center panel) color scaled to the density of molecular formulas. Each pixel on the grid of the center panel is color scaled to the number of molecular formulas at each value. The density distribution of the formulas by carbon number and DBE (top and right panels respectively) are subsequently color scaled to the number of oxygen atoms in each formula and to the modified aromaticity index (AI_{mod}) (See section 2.2). The total number of formulas are stacked in the density distribution plots.

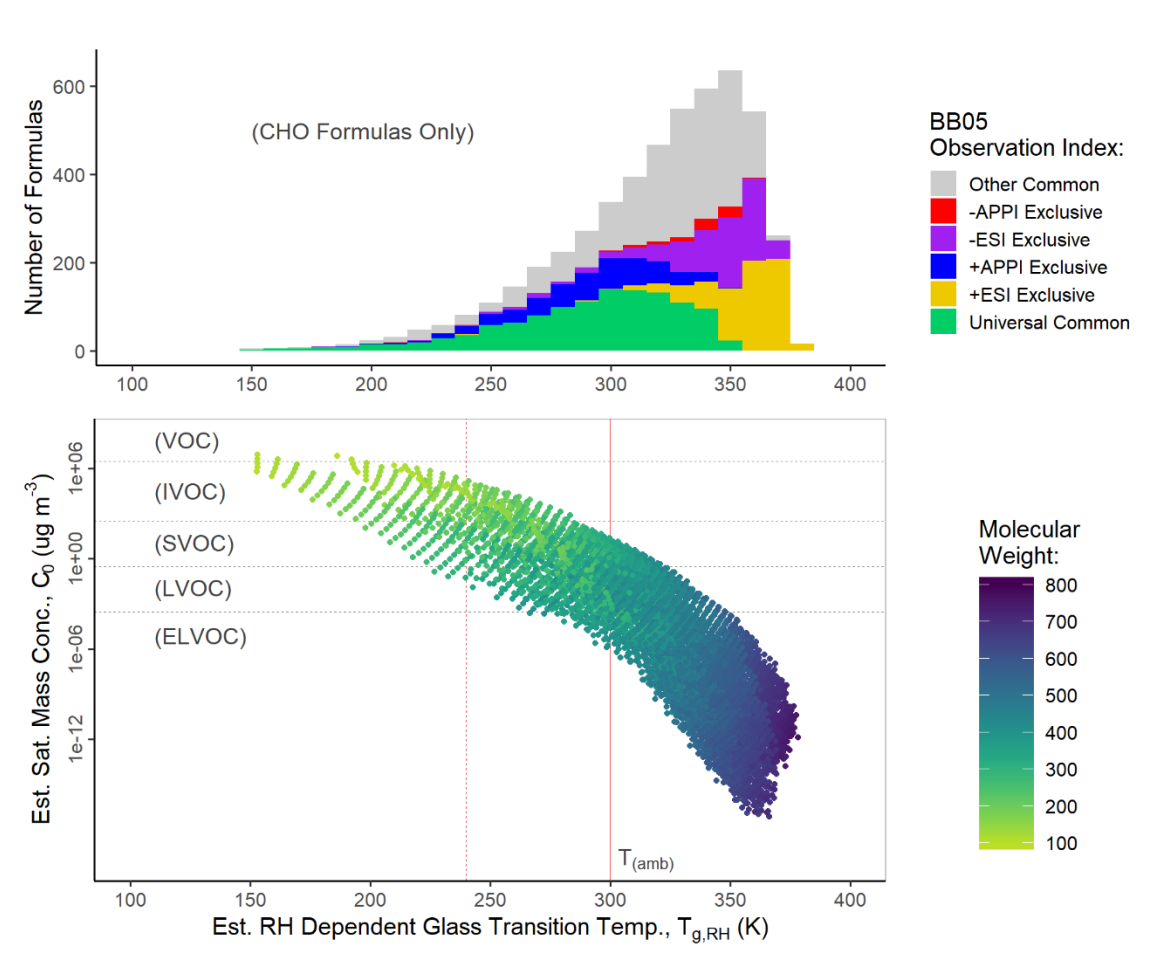


Figure 4. Distribution of CHO molecular formulas for BB05 in estimated saturation mass concentration (C_0) vs. estimated relative humidity dependent glass transition temperature ($T_{g,RH}$) space (bottom panel) (See section 2.2). The distribution of those molecular formulas by $T_{g,RH}$ (top panel) are color coded by the method of detection, whether a formula was exclusive to one of the four ionization modes (red, purple, blue, gold) detected in all four modes (green) or some other combination of multiple ionization modes (gray). The total number of formulas are stacked in the density distribution plot. The solid red line at 300 K represents the average ambient temperature (T_{amb}) during sample collection. Species with a $T_{g,RH}$ which approach or exceed T_{amb} are more likely to be in a semi-solid or solid phase respectively. The dashed red line at 240 K represents the theoretical temperature for the expected phase state ratio transition between liquid and semi-solid.

ASSOCIATED CONTENT

Data availability: The complete OTE- MS data set is available for download on Digital Commons: https://digitalcommons.mtu.edu/all-datasets/6/ (Brege et al., 2021).

Supplement: The associated supplemental text for this article is available online: [link]. The supplemental text includes a detailed synopsis of molecular formula assignment using MFAssignR, a detailed description of the calculations performed using the assigned molecular formulas, including glass transition temperature and volatility estimations, as well as the supplemental tables and figures which are referred to within this article.

AUTHOR INFORMATION

Corresponding Author

*Matthew Brege (matthew.brege@gmail.com)

Author Contributions

This study was designed by S.C., A.Z., and L.M. OTE-MS analysis and molecular formula assignments were performed by M.B. and S.S. SEM, STXM, NEXAFS, miniSPLAT and room-temperature evaporation kinetics analyses were performed by S.C. and A.Z. The manuscript was prepared by M.B.

Competing interests

The authors declare that they have no conflict of interest.

ACKNOWLEDGMENT

A portion of research was performed at Environmental Molecular Sciences Laboratory (EMSL), a national scientific user facility sponsored by the U.S. Department of Energy's (U.S. DOE) Office of Biological and Environmental Research and located at the Pacific Northwest National Laboratory (PNNL). STXM/NEXAFS analysis at beamline 5.3.2 of the Advanced Light Source at Lawrence Berkeley National Laboratory is supported by the Office of Science, and Office of Basic Energy Sciences of the U.S. Department of Energy. Support was provided by the U.S. DOE Office of Biological and Environmental Research (OBER) Atmospheric Research Systems Program (ASR). The authors thank Dr. Maryam Khaksari, previously of the Chemical Advanced Resolution Methods (ChARM) Laboratory at Michigan Technological University (Houghton, Michigan, USA) Mass Spectrometry Facility, for instrument time and assistance with OTE-MS data acquisition.

REFERENCES

- 1. Westerling, A. L.; Hidalgo, H. G.; Cayan, D. R.; Swetnam, T. W., Warming and earlier spring increase western US forest wildfire activity. *Science* **2006**, *313* (5789), 940-943.
- 2. Barbero, R.; Abatzoglou, J. T.; Larkin, N. K.; Kolden, C. A.; Stocks, B., Climate change presents increased potential for very large fires in the contiguous United States. *Int J Wildland Fire* **2015**, *24* (7), 892-899.
- 3. Gergel, D. R.; Nijssen, B.; Abatzoglou, J. T.; Lettenmaier, D. P.; Stumbaugh, M. R., Effects of climate change on snowpack and fire potential in the western USA. *Climatic Change* **2017**, *141* (2), 287-299.
- 4. Damoah, R.; Spichtinger, N.; Forster, C.; James, P.; Mattis, I.; Wandinger, U.; Beirle, S.; Wagner, T.; Stohl, A., Around the world in 17 days hemispheric-scale transport of forest fire smoke from Russia in May 2003. *Atmos Chem Phys* **2004**, *4*, 1311-1321.
- 5. Koppmann, R.; Czapiewski, K. v.; Reid, J., A review of biomass burning emissions, part I: gaseous emissions of carbon monoxide, methane, volatile organic compounds, and nitrogen containing compounds. *Atmospheric chemistry and physics discussions* **2005**, *5* (5), 10455-10516.
- 6. Yu, P.; Toon, O. B.; Bardeen, C. G.; Zhu, Y.; Rosenlof, K. H.; Portmann, R. W.; Thornberry, T. D.; Gao, R.-S.; Davis, S. M.; Wolf, E. T. J. S., Black carbon lofts wildfire smoke high into the stratosphere to form a persistent plume. **2019**, *365* (6453), 587-590.
- 7. Simoneit, B. R. T., Biomass burning A review of organic tracers for smoke from incomplete combustion. *Appl Geochem* **2002**, *17* (3), 129-162.
- 8. Fleming, L. T.; Lin, P.; Laskin, A.; Laskin, J.; Weltman, R.; Edwards, R. D.; Arora, N. K.; Yadav, A.; Meinardi, S.; Blake, D. R.; Pillarisetti, A.; Smith, K. R.; Nizkorodov, S. A.,

Molecular composition of particulate matter emissions from dung and brushwood burning household cookstoves in Haryana, India. *Atmos Chem Phys* **2018**, *18* (4), 2461-2480.

- 9. Fleming, L. T.; Weltman, R.; Yadav, A.; Edwards, R. D.; Arora, N. K.; Pillarisetti, A.; Meinardi, S.; Smith, K. R.; Blake, D. R.; Nizkorodov, S. A. J. A. C.; Physics, Emissions from village cookstoves in Haryana, India, and their potential impacts on air quality. **2018**, *18* (20), 15169-15182.
- 10. Kroll, J. H.; Seinfeld, J. H., Chemistry of secondary organic aerosol: Formation and evolution of low-volatility organics in the atmosphere. *Atmos Environ* **2008**, *42* (16), 3593-3624.
- 11. Zhang, R., Getting to the critical nucleus of aerosol formation. *Science* **2010**, *328* (5984), 1366-1367.
- 12. WHO, Ambient air pollution: A global assessment of exposure and burden of disease. **2016**.
- 13. IPCC, Global Warming of 1.5° C: An IPCC Special Report on the Impacts of Global Warming of 1.5° C Above Pre-industrial Levels and Related Global Greenhouse Gas Emission Pathways, in the Context of Strengthening the Global Response to the Threat of Climate Change, Sustainable Development, and Efforts to Eradicate Poverty. Intergovernmental Panel on Climate Change: 2018.
- 14. Harrison, M. A.; Barra, S.; Borghesi, D.; Vione, D.; Arsene, C.; Olariu, R. I. J. A. E., Nitrated phenols in the atmosphere: a review. **2005**, *39* (2), 231-248.
- 15. Farmer, P. B., Molecular epidemiology studies of carcinogenic environmental pollutants Effects of polycyclic aromatic hydrocarbons (PAHs) in environmental pollution on exogenous and oxidative DNA damage. *Mutat Res-Rev Mutat* **2003**, *544* (2-3), 397-402.
- 16. Xue, W. L.; Warshawsky, D., Metabolic activation of polycyclic and heterocyclic aromatic hydrocarbons and DNA damage: A review. *Toxicol Appl Pharm* **2005**, *206* (1), 73-93.
- 17. Lin, P.; Yu, J. Z., Generation of Reactive Oxygen Species Mediated by Humic-like Substances in Atmospheric Aerosols. *Environ Sci Technol* **2011**, *45* (24), 10362-10368.
- 18. Verma, V.; Fang, T.; Xu, L.; Peltier, R. E.; Russell, A. G.; Ng, N. L.; Weber, R. J., Organic Aerosols Associated with the Generation of Reactive Oxygen Species (ROS) by Water-Soluble PM2.5. *Environ Sci Technol* **2015**, *49* (7), 4646-4656.
- 19. Andreae, M. O.; Gelencser, A., Black carbon or brown carbon? The nature of light-absorbing carbonaceous aerosols. *Atmos Chem Phys* **2006**, *6*, 3131-3148.
- 20. Saleh, R.; Cheng, Z. Z.; Atwi, K., The Brown-Black Continuum of Light-Absorbing Combustion Aerosols. *Environ Sci Tech Let* **2018**, *5* (8), 508-513.
- 21. Chow, J. C.; Watson, J. G.; Green, M. C.; Wang, X.; Chen, L. W. A.; Trimble, D. L.; Cropper, P. M.; Kohl, S. D.; Gronstal, S. B., Separation of brown carbon from black carbon for IMPROVE and Chemical Speciation Network PM2.5 samples. *J Air Waste Manage* **2018**, *68* (5), 494-510.
- 22. Phillips, S. M.; Smith, G. D., Light Absorption by Charge Transfer Complexes in Brown Carbon Aerosols. *Environ Sci Tech Let* **2014**, *I* (10), 382-386.
- 23. Phillips, S. M.; Smith, G. D., Further Evidence for Charge Transfer Complexes in Brown Carbon Aerosols from Excitation-Emission Matrix Fluorescence Spectroscopy. *J Phys Chem A* **2015**, *119* (19), 4545-4551.
- 24. Reid, J. S.; Eck, T. F.; Christopher, S. A.; Koppmann, R.; Dubovik, O.; Eleuterio, D. P.; Holben, B. N.; Reid, E. A.; Zhang, J., A review of biomass burning emissions part III: intensive optical properties of biomass burning particles. *Atmos. Chem. Phys.* **2005**, *5* (3), 827-849.

- 25. Sengupta, D.; Samburova, V.; Bhattarai, C.; Kirillova, E.; Mazzoleni, L.; Iaukea-Lum, M.; Watts, A.; Moosmüller, H.; Khlystov, A., Light absorption by polar and non-polar aerosol compounds from laboratory biomass combustion. *Atmos. Chem. Phys.* **2018**, *18* (15), 10849-10867.
- 26. Bond, T. C.; Streets, D. G.; Yarber, K. F.; Nelson, S. M.; Woo, J. H.; Klimont, Z., A technology-based global inventory of black and organic carbon emissions from combustion. *J Geophys Res-Atmos* **2004**, *109* (D14), D14203.
- 27. Jacobson, M. Z., Control of fossil-fuel particulate black carbon and organic matter, possibly the most effective method of slowing global warming. *J Geophys Res-Atmos* **2002**, *107* (D19).
- 28. Kanakidou, M.; Seinfeld, J. H.; Pandis, S. N.; Barnes, I.; Dentener, F. J.; Facchini, M. C.; Van Dingenen, R.; Ervens, B.; Nenes, A.; Nielsen, C. J.; Swietlicki, E.; Putaud, J. P.; Balkanski, Y.; Fuzzi, S.; Horth, J.; Moortgat, G. K.; Winterhalter, R.; Myhre, C. E. L.; Tsigaridis, K.; Vignati, E.; Stephanou, E. G.; Wilson, J., Organic aerosol and global climate modelling: a review. *Atmos. Chem. Phys.* **2005**, *5* (4), 1053-1123.
- 29. Reid, J. S.; Koppmann, R.; Eck, T. F.; Eleuterio, D. P., A review of biomass burning emissions part II: intensive physical properties of biomass burning particles. *Atmos Chem Phys* **2005**, *5*, 799-825.
- 30. Reid, J. P.; Bertram, A. K.; Topping, D. O.; Laskin, A.; Martin, S. T.; Petters, M. D.; Pope, F. D.; Rovelli, G., The viscosity of atmospherically relevant organic particles. *Nat Commun* **2018**, *9*.
- 31. Sedlacek, A. J.; Buseck, P. R.; Adachi, K.; Onasch, T. B.; Springston, S. R.; Kleinman, L., Formation and evolution of tar balls from northwestern US wildfires. *Atmos Chem Phys* **2018**, *18* (15), 11289-11301.
- 32. Posfai, M.; Gelencser, A.; Simonics, R.; Arato, K.; Li, J.; Hobbs, P. V.; Buseck, P. R., Atmospheric tar balls: Particles from biomass and biofuel burning. *J Geophys Res-Atmos* **2004**, *109* (D6).
- 33. Chakrabarty, R. K.; Moosmuller, H.; Chen, L. W. A.; Lewis, K.; Arnott, W. P.; Mazzoleni, C.; Dubey, M. K.; Wold, C. E.; Hao, W. M.; Kreidenweis, S. M., Brown carbon in tar balls from smoldering biomass combustion. *Atmos Chem Phys* **2010**, *10* (13), 6363-6370.
- 34. China, S.; Mazzoleni, C.; Gorkowski, K.; Aiken, A. C.; Dubey, M. K., Morphology and mixing state of individual freshly emitted wildfire carbonaceous particles. *Nat Commun* **2013**, *4*.
- 35. Adachi, K.; Sedlacek, A. J.; Kleinman, L.; Springston, S. R.; Wang, J.; Chand, D.; Hubbe, J. M.; Shilling, J. E.; Onasch, T. B.; Kinase, T. J. P. o. t. N. A. o. S., Spherical tarball particles form through rapid chemical and physical changes of organic matter in biomass-burning smoke. **2019**, 201900129.
- 36. Alexander, D. T. L.; Crozier, P. A.; Anderson, J. R., Brown carbon spheres in East Asian outflow and their optical properties. *Science* **2008**, *321* (5890), 833-836.
- 37. Bhandari, J., Morphology and mixing state of soot and tar balls: implications for optical properties and climate. *Open Access Dissertation, Michigan Technological University* **2018**.
- 38. Wielgosiński, G., Pollutant formation in combustion processes. In *Advances in Chemical Engineering*, IntechOpen: 2012.
- 39. Andreae, M. O.; Merlet, P., Emission of trace gases and aerosols from biomass burning. *Global Biogeochem Cy* **2001,** *15* (4), 955-966.

- 40. Mazzoleni, L. R.; Zielinska, B.; Moosmuller, H., Emissions of levoglucosan, methoxy phenols, and organic acids from prescribed burns, laboratory combustion of wildland fuels, and residential wood combustion. *Environ Sci Technol* **2007**, *41* (7), 2115-2122.
- 41. Samburova, V.; Connolly, J.; Gyawali, M.; Yatavelli, R. L. N.; Watts, A. C.; Chakrabarty, R. K.; Zielinska, B.; Moosmuller, H.; Khlystov, A., Polycyclic aromatic hydrocarbons in biomass-burning emissions and their contribution to light absorption and aerosol toxicity. *Sci Total Environ* **2016**, *568*, 391-401.
- 42. Li, C. L.; He, Q. F.; Schade, J.; Passig, J.; Zimmermann, R.; Meidan, D.; Laskin, A.; Rudich, Y., Dynamic changes in optical and chemical properties of tar ball aerosols by atmospheric photochemical aging. *Atmos Chem Phys* **2019**, *19* (1), 139-163.
- 43. Marshall, A. G., Milestones in Fourier transform ion cyclotron resonance mass spectrometry technique development. *Int J Mass Spectrom* **2000**, *200* (1-3), 331-356.
- 44. Zubarev, R. A.; Makarov, A., Orbitrap Mass Spectrometry. *Anal Chem* **2013**, *85* (11), 5288-5296.
- 45. Konermann, L.; Ahadi, E.; Rodriguez, A. D.; Vahidi, S., Unraveling the Mechanism of Electrospray Ionization. *Anal Chem* **2013**, *85* (1), 2-9.
- 46. Altieri, K. E.; Turpin, B. J.; Seitzinger, S. P., Oligomers, organosulfates, and nitrooxy organosulfates in rainwater identified by ultra-high resolution electrospray ionization FT-ICR mass spectrometry. *Atmos Chem Phys* **2009**, *9* (7), 2533-2542.
- 47. Schmitt-Kopplin, P.; Gelencser, A.; Dabek-Zlotorzynska, E.; Kiss, G.; Hertkorn, N.; Harir, M.; Hong, Y.; Gebefugi, I., Analysis of the Unresolved Organic Fraction in Atmospheric Aerosols with Ultrahigh-Resolution Mass Spectrometry and Nuclear Magnetic Resonance Spectroscopy: Organosulfates As Photochemical Smog Constituents. *Anal Chem* **2010**, 82 (19), 8017-8026.
- 48. Lin, P.; Rincon, A. G.; Kalberer, M.; Yu, J. Z., Elemental Composition of HULIS in the Pearl River Delta Region, China: Results Inferred from Positive and Negative Electrospray High Resolution Mass Spectrometric Data. *Environ Sci Technol* **2012**, *46* (14), 7454-7462.
- 49. Zhao, Y.; Hallar, A. G.; Mazzoleni, L. R., Atmospheric organic matter in clouds: exact masses and molecular formula identification using ultrahigh-resolution FT-ICR mass spectrometry. *Atmos Chem Phys* **2013**, *13* (24), 12343-12362.
- 50. Wozniak, A. S.; Willoughby, A. S.; Gurganus, S. C.; Hatcher, P. G., Distinguishing molecular characteristics of aerosol water soluble organic matter from the 2011 trans-North Atlantic US GEOTRACES cruise. *Atmos Chem Phys* **2014**, *14* (16), 8419-8434.
- 51. Dzepina, K.; Mazzoleni, C.; Fialho, P.; China, S.; Zhang, B.; Owen, R. C.; Helmig, D.; Hueber, J.; Kumar, S.; Perlinger, J. A.; Kramer, L. J.; Dziobak, M. P.; Ampadu, M. T.; Olsen, S.; Wuebbles, D. J.; Mazzoleni, L. R., Molecular characterization of free tropospheric aerosol collected at the Pico Mountain Observatory: a case study with a long-range transported biomass burning plume. *Atmos Chem Phys* **2015**, *15* (9), 5047-5068.
- 52. Willoughby, A. S.; Wozniak, A. S.; Hatcher, P. G., Detailed Source-Specific Molecular Composition of Ambient Aerosol Organic Matter Using Ultrahigh Resolution Mass Spectrometry and H-1 NMR. *Atmosphere-Basel* **2016**, *7*(6), 79.
- 53. Cook, R. D.; Lin, Y. H.; Peng, Z. Y.; Boone, E.; Chu, R. K.; Dukett, J. E.; Gunsch, M. J.; Zhang, W. L.; Tolic, N.; Laskin, A.; Pratt, K. A., Biogenic, urban, and wildfire influences on the molecular composition of dissolved organic compounds in cloud water. *Atmos Chem Phys* **2017**, *17* (24), 15167-15180.

- 54. Kauppila, T. J.; Kuuranne, T.; Meurer, E. C.; Eberlin, M. N.; Kotiaho, T.; Kostiainen, R., Atmospheric pressure photoionization mass spectrometry. Ionization mechanism and the effect of solvent on the ionization of naphthalenes. *Anal Chem* **2002**, *74* (21), 5470-5479.
- 55. NWCC Northwest Annual Fire Report 2017; 2018.
- 56. Tfaily, M. M.; Chu, R. K.; Tolic, N.; Roscioli, K. M.; Anderton, C. R.; Pasa-Tolic, L.; Robinson, E. W.; Hess, N. J., Advanced Solvent Based Methods for Molecular Characterization of Soil Organic Matter by High-Resolution Mass Spectrometry. *Anal Chem* **2015**, *87* (10), 5206-5215.
- 57. Schum, S. K.; Brown, L. E.; Mazzoleni, L. R., MFAssignR: Molecular formula assignment software for ultrahigh resolution mass spectrometry analysis of environmental complex mixtures. *Environ Res* **2020**, *191*, 110114.
- 58. Brege, M.; Paglione, M.; Gilardoni, S.; Decesari, S.; Facchini, M. C.; Mazzoleni, L. R., Molecular insights on aging and aqueous-phase processing from ambient biomass burning emissions-influenced Po Valley fog and aerosol. *Atmos Chem Phys* **2018**, *18* (17), 13197-13214.
- 59. Schum, S. K.; Zhang, B.; Dzepina, K.; Fialho, P.; Mazzoleni, C.; Mazzoleni, L. R., Molecular and physical characteristics of aerosol at a remote free troposphere site: implications for atmospheric aging. *Atmos Chem Phys* **2018**, *18* (19), 14017-14036.
- 60. Zark, M.; Christoffers, J.; Dittmar, T., Molecular properties of deep-sea dissolved organic matter are predictable by the central limit theorem: Evidence from tandem FT-ICR-MS. *Mar Chem* **2017**, *191*, 9-15.
- 61. Hawkes, J. A.; Patriarca, C.; Sjoberg, P. J. R.; Tranvik, L.; Bergquist, J., Extreme isomeric complexity of dissolved organic matter found across aquatic environments. *Limnology and Oceanography Letters* **2018**, *3* (2), 21-30.
- 62. Koch, B. P.; Dittmar, T., From mass to structure: an aromaticity index for high-resolution mass data of natural organic matter. *Rapid Commun Mass Sp* **2006**, *20* (5), 926-932.
- 63. Koch, B. P.; Dittmar, T., From mass to structure: an aromaticity index for high-resolution mass data of natural organic matter (vol 20, pg 926, 2006). *Rapid Commun Mass Sp* **2016**, *30* (1), 250-250.
- 64. Kroll, J. H.; Donahue, N. M.; Jimenez, J. L.; Kessler, S. H.; Canagaratna, M. R.; Wilson, K. R.; Altieri, K. E.; Mazzoleni, L. R.; Wozniak, A. S.; Bluhm, H.; Mysak, E. R.; Smith, J. D.; Kolb, C. E.; Worsnop, D. R., Carbon oxidation state as a metric for describing the chemistry of atmospheric organic aerosol. *Nat Chem* **2011**, *3* (2), 133-139.
- 65. Li, Y.; Poschl, U.; Shiraiwa, M., Molecular corridors and parameterizations of volatility in the chemical evolution of organic aerosols. *Atmos Chem Phys* **2016**, *16* (5), 3327-3344.
- 66. Vaden, T. D.; Imre, D.; Beranek, J.; Shrivastava, M.; Zelenyuk, A., Evaporation kinetics and phase of laboratory and ambient secondary organic aerosol. *P Natl Acad Sci USA* **2011**, *108* (6), 2190-2195.
- 67. DeRieux, W. S.; Li, Y.; Lin, P.; Laskin, J.; Laskin, A.; Bertram, A. K.; Nizkorodov, S. A.; Shiraiwa, M., Predicting the glass transition temperature and viscosity of secondary organic material using molecular composition. *Atmos Chem Phys* **2018**, *18* (9), 6331-6351.
- 68. Zelenyuk, A.; Imre, D.; Wilson, J.; Zhang, Z. Y.; Wang, J.; Mueller, K., Airborne Single Particle Mass Spectrometers (SPLAT II & miniSPLAT) and New Software for Data Visualization and Analysis in a Geo-Spatial Context. *J Am Soc Mass Spectr* **2015**, *26* (2), 257-270.

- 69. Tivanski, A. V.; Hopkins, R. J.; Tyliszczak, T.; Gilles, M. K., Oxygenated interface on biomass burn tar balls determined by single particle scanning transmission X-ray microscopy. *J Phys Chem A* **2007**, *111* (25), 5448-5458.
- 70. Lin, P.; Fleming, L. T.; Nizkorodov, S. A.; Laskin, J.; Laskin, A., Comprehensive Molecular Characterization of Atmospheric Brown Carbon by High Resolution Mass Spectrometry with Electrospray and Atmospheric Pressure Photoionization. *Anal Chem* **2018**, *90* (21), 12493-12502.
- 71. Cech, N. B.; Enke, C. G., Practical implications of some recent studies in electrospray ionization fundamentals. *Mass Spectrom Rev* **2001**, *20* (6), 362-387.
- 72. Tu, P. J.; Hall, W. A.; Johnston, M. V., Characterization of Highly Oxidized Molecules in Fresh and Aged Biogenic Secondary Organic Aerosol. *Anal Chem* **2016**, 88 (8), 4495-4501.
- 73. Hinks, M. L.; Brady, M. V.; Lignell, H.; Song, M. J.; Grayson, J. W.; Bertram, A. K.; Lin, P.; Laskin, A.; Laskin, J.; Nizkorodov, S. A., Effect of viscosity on photodegradation rates in complex secondary organic aerosol materials. *Phys Chem Chem Phys* **2016**, *18* (13), 8785-8793.
- 74. Alves, C. A.; Vicente, A. M.; Custodio, D.; Cerqueira, M.; Nunes, T.; Pio, C.; Lucarelli, F.; Calzolai, G.; Nava, S.; Diapouli, E.; Eleftheriadis, K.; Querol, X.; Bandowe, B. A. M., Polycyclic aromatic hydrocarbons and their derivatives (nitro-PAHs, oxygenated PAHs, and azaarenes) in PM2.5 from Southern European cities. *Sci Total Environ* **2017**, *595*, 494-504. 75. Shimizu, M.; Yano, E., Mutagenicity of Mono-Nitrobenzene Derivatives in the Ames
- Test and Rec Assay. *Mutat Res* **1986,** *170* (1-2), 11-22.
- 76. Yu, L.; Smith, J.; Laskin, A.; George, K. M.; Anastasio, C.; Laskin, J.; Dillner, A. M.; Zhang, Q., Molecular transformations of phenolic SOA during photochemical aging in the aqueous phase: competition among oligomerization, functionalization, and fragmentation. *Atmos Chem Phys* **2016**, *16* (7), 4511-4527.
- 77. Lin, P.; Bluvshtein, N.; Rudich, Y.; Nizkorodov, S. A.; Laskin, J.; Laskin, A., Molecular Chemistry of Atmospheric Brown Carbon Inferred from a Nationwide Biomass Burning Event. *Environ Sci Technol* **2017**, *51* (20), 11561-11570.
- 78. Hawkins, L.; Welsh, H.; Alexander, M., Evidence for pyrazine-based chromophores in cloudwater mimics containing methylglyoxal and ammonium sulfate. *Atmos. Chem. Phys. Discuss.* **2018**, 29.
- 79. Mazzoleni, L. R.; Saranjampour, P.; Dalbec, M. M.; Samburova, V.; Hallar, A. G.; Zielinska, B.; Lowenthal, D. H.; Kohl, S., Identification of water-soluble organic carbon in non-urban aerosols using ultrahigh-resolution FT-ICR mass spectrometry: organic anions. *Environ Chem* **2012**, *9* (3), 285-297.
- 80. Kourtchev, I.; O'Connor, I. P.; Giorio, C.; Fuller, S. J.; Kristensen, K.; Maenhaut, W.; Wenger, J. C.; Sodeau, J. R.; Glasius, M.; Kalberer, M., Effects of anthropogenic emissions on the molecular composition of urban organic aerosols: An ultrahigh resolution mass spectrometry study. *Atmos Environ* **2014**, *89*, 525-532.
- 81. Wang, X. K.; Hayeck, N.; Bruggemann, M.; Yao, L.; Chen, H. F.; Zhang, C.; Emmelin, C.; Chen, J. M.; George, C.; Wang, L., Chemical Characteristics of Organic Aerosols in Shanghai: A Study by Ultrahigh-Performance Liquid Chromatography Coupled With Orbitrap Mass Spectrometry. *J Geophys Res-Atmos* **2017**, *122* (21), 11703-11722.

For Table of Contents Only

